

Design of Novel Bilayer Compounds of the CPO-8 Type Containing 1D Channels

Kjell Ove Kongshaug and Helmer Fjellvåg*

Department of Chemistry, University of Oslo, P.O. Box 1033 Blindern, N-0315 Oslo, Norway

Received April 29, 2005

The reaction between $\text{Zn}(\text{NO}_3)_2 \cdot 6\text{H}_2\text{O}$ and 5-aminoisophthalic acid (aip) in a mixture of diethylformamide (DEF) and ethanol resulted in $[\text{Zn}(\text{C}_8\text{H}_5\text{NO}_4)(\text{C}_5\text{H}_{11}\text{NO})]_n$ (CPO-8-DEF). This compound is composed of infinite 2D layers with tetrahedral Zn atoms and aip ligands in a triangular topology. The DEF molecules are bonded to Zn, and within each layer, the DEF molecules are oriented in the same direction, while in the subsequent layer, the DEF molecules are oriented in the opposite direction. By introduction of the pillaring ligands 4,4'-bipyridine (BPY), 1,2-di-4-pyridylethylene (DPE), 1,2-di-4-pyridylethane (DPA), and 1,3-di-4-pyridylpropane (DPP) into mixtures of *N,N'*-dimethylformamide and water with $\text{Zn}(\text{NO}_3)_2$ and aip, we have successfully synthesized a series of related pillared bilayer compounds with the same common triangular $\text{Zn}(\text{aip})$ layer structural motif as that observed in CPO-8-DEF. The compounds are denoted as CPO-8-BPY ($[\text{Zn}(\text{C}_8\text{H}_5\text{NO}_4)(\text{C}_{10}\text{H}_8\text{N}_2)_{0.5}]_n \cdot 3n\text{H}_2\text{O}$), CPO-8-DPE ($[\text{Zn}(\text{C}_8\text{H}_5\text{NO}_4)(\text{C}_{12}\text{H}_{10}\text{N}_2)_{0.5}]_n \cdot 2.5n\text{H}_2\text{O}$), CPO-8-DPA ($[\text{Zn}(\text{C}_8\text{H}_5\text{NO}_4)(\text{C}_{12}\text{H}_{12}\text{N}_2)_{0.5}]_n \cdot 2.5n\text{H}_2\text{O}$), and CPO-8-DPP ($[\text{Zn}(\text{C}_8\text{H}_5\text{NO}_4)(\text{C}_{13}\text{H}_{14}\text{N}_2)_{0.5}]_n \cdot 3n\text{H}_2\text{O}$). In all cases, the pillars create spaces inside the bilayers that result in 1D channels running along the [010] directions with dimensions of $3.5 \times 6.7 \text{ \AA}^2$. These channels contain water molecules that can be removed on heating to $150 \text{ }^\circ\text{C}$, resulting in porous structures. The crystal structures of these porous high-temperature variants have been determined on the basis of powder X-ray diffraction data. All of the compounds show preferential adsorption of H_2 over N_2 at 77 K .

Introduction

The construction of polymeric metal–organic frameworks (MOFs) is currently attracting considerable attention because of the possible application for such compounds in areas such as separation, catalysis, ion exchange, and gas storage.^{1–11}

The MOF type of compounds offers great scope for the rational design of solids with pores of defined size, shape, and chemical environment. This represents the so-called bottom-up method. However, synthetic chemistry is not yet developed to a stage where pore structures can be designed. Hence, the exploratory synthetic approach is still ruling the field, where the discovery of novel compounds is mostly serendipitous using methods referred to by critics as “shake and bake” or “mix and wait”. A great motivation is thus to develop controlled synthetic techniques for these extreme complex systems.

Recently, the concept of the secondary building unit (SBU) has been advanced for the understanding and prediction of the topologies of MOF structures. Yaghi and co-workers¹² have defined the concept of reticular synthesis, indicating topological rules that govern the design of MOF types of compounds. These concepts start from the existence of well-defined inorganic SBUs and organic linker molecules that maintain their structural integrity throughout the construction

* To whom correspondence should be addressed. E-mail: helmer.fjellvag@kjemi.uio.no. Tel: +4722855564. Fax: +4722855565.

- (1) Yaghi, O. M.; Davis, C. E.; Li, G. M.; Li, H. L. *J. Am. Chem. Soc.* **1997**, *119*, 2861.
- (2) Seo, J. S.; Whang, D.; Lee, H.; Jun, S. I.; Oh, J.; Jeon, Y. J.; Kim, K. *Nature* **2000**, *404*, 982.
- (3) Bennett, M. V.; Shores, M. P.; Beauvais, L. G.; Long, J. R. *J. Am. Chem. Soc.* **2000**, *122*, 6664.
- (4) Blom, R.; Heyn, R. H.; Swang, O.; Fjellvåg, H.; Kongshaug, K. O.; Nielsen, R. K. B. *Chem. Eng. Trans.* **2004**, *4*, 325.
- (5) Janiak, C. *Dalton Trans.* **2003**, 2781.
- (6) Mori, W.; Takamizawa, S.; Kato, C. N.; Ohmura, T.; Sato, T. *Microporous Mesoporous Mater.* **2004**, *73*, 31.
- (7) Rosseinsky, M. J. *Microporous Mesoporous Mater.* **2004**, *73*, 15.
- (8) Ferey, G.; Mellot-Draznieks, C.; Serre, C.; Millange, F. *Acc. Chem. Res.* **2005**, *38*, 217.
- (9) Ferey, G.; Mellot-Draznieks, C.; Serre, C.; Millange, F.; Dutour, J.; Surble, S.; Margiolaki, I. *Science* **2005**, *309*, 2040.
- (10) Kitagawa, S.; Uemura, K. *Chem. Soc. Rev.* **2005**, *34*, 109.
- (11) Rowsell, J. L. C.; Yaghi, O. M. *Angew. Chem., Int. Ed.* **2005**, *44*, 4670.

- (12) Yaghi, O. M.; O’Keeffe, M.; Ockwig, N. W.; Chae, H. K.; Eddaoudi, M.; Kim, J. *Nature* **2003**, *423*, 705.

process of the solid. Different combinations of inorganic SBUs and organic linker molecules may assemble by strong bonding to ordered structures showing topologies of dense structures. Ferey and co-workers¹³ have developed these concepts further by the introduction of a computational approach for the enumeration of the possible frameworks accessible from the building blocks. They proved the strength of the method by being able to define structures known in the literature by starting from their organic and inorganic building blocks, and, interestingly, they also predicted topologies for which no material is yet synthesized.

In the concept of reticular synthesis of porous MOF structures, the inorganic SBUs tend to consist of a limited number of metal centers. However, larger structural motifs might also lead to porous MOF structures. In particular, 2D-layered structural motifs can be pillared into 3D porous pillared layer structures. This approach has been applied by Kitagawa et al.,¹⁴ Seki and Mori,¹⁵ and Kim et al.¹⁶ to obtain 3D porous MOF compounds. Clearfield and co-workers have also used this approach to produce porous zirconium diphosphate compounds.^{17,18} Such synthetic systems might be very attractive because they enable possible control of both the pore size and chemical functionality of the pores via modification of the pillar module.

In this paper, we present a synthetic system that provides a structure type denoted as CPO-8. Four different pillars have been introduced into the system, all leading to this structure type that consists of porous pillared bilayers with 1D channels.

Experimental Section

All syntheses were performed in Teflon-lined steel autoclaves under autogenous pressure. Reagents were purchased commercially and used without further purification. Thermogravimetric analysis (TGA) measurements were carried out on a Perkin-Elmer thermogravimetric analyzer in a N₂ gas stream using a heating rate of 5 °C/min. The N₂ and H₂ gas sorption isotherm measurements were carried out at 77 K. The experiments for N₂ were performed using a BELSORP mini instrument, while the H₂ experiments were done using a Quantachrome Autosorb-1 instrument. Prior to the measurements, the samples were dried under a high vacuum at 150 °C for 18 h to remove the solvated water molecules.

For all compounds, Zn(NO₃)₂·6H₂O (179 mg, 0.6 mmol) and 5-aminoisophthalic acid (aip; 110 mg, 0.6 mmol) were used as reagents. The light-brown crystalline products (brown for CPO-8-DEF) were washed with water (DEF for CPO-8-DEF) and dried in air at room temperature. Additional specific information is given in the following:

Synthesis of [Zn(C₈H₅NO₄)(C₅H₁₁NO)]_n (CPO-8-DEF). The reagent mixture along with ethanol (2.5 mL) and diethylformamide (DEF; 7.5 mL) was heated to 95 °C for 24 h. The yield was 65%

based on Zn. Anal. Calcd for C₁₃H₁₆N₂O₅Zn (%): C, 45.17; H, 4.66; N, 8.11. Found (%): C, 44.27; H, 4.56; N, 8.02.

Synthesis of [Zn(C₈H₅NO₄)(C₁₀H₈N₂)_{0.5}]_n·3nH₂O (CPO-8-BPY). The reagent mixture along with 4,4'-bipyridine (BPY; 0.094 g, 0.6 mmol), *N,N'*-dimethylformamide (DMF; 8.0 mL), and water (8.0 mL) was heated to 120 °C for 24 h. The yield was 70% based on Zn. Anal. Calcd for C₁₃H₁₅N₂O₇Zn (%): C, 41.45; H, 4.01; N, 7.43. Found (%): C, 43.09; H, 3.63; N, 7.18.

Synthesis of [Zn(C₈H₅NO₄)(C₁₂H₁₀N₂)_{0.5}]_n·2.5nH₂O (CPO-8-DPE). The reagent mixture along with 1,2-di-4-pyridylethylene (DPE; 0.109 g, 0.6 mmol), DMF (8.0 mL), and water (8.0 mL) was heated to 105 °C for 24 h. The yield was 60% based on Zn. Anal. Calcd for C₂₈H₃₀N₄O₁₃Zn₂ (%): C, 44.17; H, 3.97; N, 7.36. Found (%): C, 44.60; H, 3.81; N, 7.09.

Synthesis of [Zn(C₈H₅NO₄)(C₁₂H₁₂N₂)_{0.5}]_n·2.5nH₂O (CPO-8-DPA). The reagent mixture along with 1,2-di-4-pyridylethane (DPA; 0.111 g, 0.6 mmol), DMF (8.0 mL), and water (8.0 mL) was heated to 120 °C for 24 h. The yield was 55% based on Zn. Anal. Calcd for C₂₈H₃₂N₄O₁₃Zn₂ (%): C, 44.05; H, 4.22; N, 7.34. Found (%): C, 45.10; H, 3.95; N, 7.11.

Synthesis of [Zn(C₈H₅NO₄)(C₁₃H₁₄N₂)_{0.5}]_n·3nH₂O (CPO-8-DPP). The reagent mixture along with 1,3-di-4-pyridylpropane (DPP; 0.357 g, 1.8 mmol), DMF (8.0 mL), and water (8.0 mL) was heated to 100 °C for 24 h. The yield was 50% based on Zn. Anal. Calcd for C₂₉H₃₆N₄O₁₄Zn₂ (%): C, 43.78; H, 4.56; N, 7.04. Found (%): C, 44.25; H, 4.23; N, 6.90.

Single-Crystal X-ray Diffraction Analysis. Single-crystal X-ray diffraction data for the CPO-8 type compounds were collected at room temperature on a Siemens diffractometer equipped with a Bruker-Nonius ApexII CCD detector. Data reduction and empirical absorption correction were carried out using the programs *SAINT*¹⁹ and *SADABS*,²⁰ respectively. The crystal structures were solved by direct methods and refined using the WinGX program.²¹ Non-H atoms were refined anisotropically. The organic H atoms were generated geometrically and refined in the riding mode. The refinements for the structures CPO-8-DEF and CPO-8-DPA ended in relatively high reliability factors (0.089 and 0.114), despite several data collections on different crystals. The crystallographic data and details on the refinements for all compounds are listed in Table 1.

Powder X-ray Diffraction Analysis. Powder X-ray diffraction data for all of the dehydrated CPO-8 type compounds (except CPO-8-DEF) were collected in transmission mode with a Siemens D5000 diffractometer using Cu Kα₁ (λ = 1.540 598 Å) radiation selected with an incident-beam germanium monochromator. The detector was a Braun position-sensitive detector. The samples were dehydrated at 150 °C for 8 h, and then they were kept in a 0.5-mm-diameter sealed borosilicate capillary. The diffraction patterns were collected over 24 h for the 2θ range of 5–80°.

The diffraction patterns were all indexed from the first 20 Bragg reflections with the program TREOR-90.²² In all cases, the unit cell dimensions are quite similar to those of the as-synthesized compounds, and hence good starting models for the structures could be built. By means of the Accelrys software, the water molecules were removed from the structure descriptions. The starting models were transferred into the GSAS program²³ for Rietveld analysis. Refinements of scale, background, zero point, and unit cell

(13) Mellot-Draznieks, C.; Dutour, J.; Ferey, G. *Angew. Chem., Int. Ed.* **2004**, *43*, 6290.

(14) Kitagawa, S.; Kitaura, R.; Noro, S. *Angew. Chem., Int. Ed.* **2004**, *43*, 2334.

(15) Seki, K.; Mori, W. *J. Phys. Chem. B* **2002**, *106*, 1380.

(16) Dybtsev, D. N.; Chun, H.; Kim, K. *Angew. Chem., Int. Ed.* **2004**, *43*, 5033.

(17) Wang, Z.; Heising, J. M.; Clearfield, A. *J. Am. Chem. Soc.* **2003**, *125*, 10375.

(18) Clearfield, A.; Wang, Z. *J. Chem. Soc., Dalton Trans.* **2002**, 2937.

(19) *SAINT*, version 7.06a; Bruker AXS Inc.: Madison, WI.

(20) *SADABS*, version 2.10; Bruker AXS Inc.: Madison, WI.

(21) Farrugia, L. J. *J. Appl. Crystallogr.* **1999**, *32*, 837.

(22) Werner, P. E.; Eriksson, L.; Westdahl, J. *J. Appl. Crystallogr.* **1985**, *18*, 367.

(23) Larson, A. C.; von Dreele, R. B. Los Alamos National Laboratory Report LA-UR-86-784; Los Alamos National Laboratory: Los Alamos, NM, 1987.

Table 1. Crystal and Structure Refinement Data for CPO-8-Type Compounds^a

	CPO-8-DEF	CPO-8-BPY	CPO-8-DPE	CPO-8-DPA	CPO-8-DPP
formula	C ₁₃ H ₁₆ N ₂ O ₅ Zn	C ₁₃ H ₁₅ N ₂ O ₇ Zn	C ₂₈ H ₃₀ N ₄ O ₁₃ Zn ₂	C ₂₈ H ₃₂ N ₄ O ₁₃ Zn ₂	C ₂₉ H ₃₆ N ₄ O ₁₄ Zn ₂
fw	345.65	376.64	761.30	763.32	795.36
T (K)	298	298	298	298	298
cryst syst	monoclinic	monoclinic	monoclinic	monoclinic	orthorhombic
space group	<i>P2₁/c</i>	<i>P2₁/c</i>	<i>C2/c</i>	<i>C2/c</i>	<i>Pna2₁</i>
<i>a</i> (Å)	11.2615(18)	12.4676(9)	26.5106(19)	26.544(6)	16.205(4)
<i>b</i> (Å)	7.6501(12)	7.6792(6)	7.4518(5)	7.4487(16)	7.6783(16)
<i>c</i> (Å)	16.284(3)	16.1832(12)	16.3890(12)	16.339(4)	25.247(5)
α (deg)	90	90	90	90	90
β (deg)	92.921(5)	108.963(2)	114.0290(10)	113.588(5)	90
γ (deg)	90	90	90	90	90
<i>V</i> (Å ³)	1401.0(4)	1465.31(19)	2957.1(4)	2960.6(11)	3141.2(12)
<i>Z</i>	4	4	4	4	4
<i>D_c</i> (g/cm ³)	1.639	1.707	1.710	1.713	1.682
μ (mm ⁻¹)	1.776	1.716	1.699	1.697	1.606
θ _{min} , θ _{max} (deg)	1.81, 23.26	1.73, 26.51	1.68, 26.41	1.67, 27.24	1.61, 20.81
no. of reflns	13989	18034	16594	19000	23654
no. of unique reflns (<i>R_{int}</i>)	2015 (0.0983)	3021 (0.0360)	3000 (0.0353)	3268 (0.0406)	3288 (0.1873)
no. of obsd reflns [<i>I</i> > 2σ(<i>I</i>)]	1242	2394	2501	2789	3288
no. of param	208	219	213	213	442
GOF	0.956	1.056	1.058	1.088	0.923
<i>R</i> ₁ , <i>wR</i> ₂ [<i>I</i> > 2σ(<i>I</i>)]	0.0478, 0.1177	0.0377, 0.0933	0.0317, 0.0825	0.0404, 0.1034	0.0573, 0.1298
<i>R</i> ₁ , <i>wR</i> ₂ (all data)	0.0890, 0.1332	0.0510, 0.1007	0.0417, 0.0866	0.0486, 0.1085	0.1138, 0.1494
Δρ (e/Å ³)	0.496, -0.647	0.847, -0.824	0.691, -0.581	0.684, -0.615	0.312, -0.699

^a The calculated standard deviations are given in parentheses.

Table 2. Experimental Conditions and Relevant Data for Rietveld Refinements of CPO-8 Types of Compounds at 150 °C^a

	CPO-8-BPY-150	CPO-8-DPE-150	CPO-8-DPA-150	CPO-8-DPP-150
formula	C ₁₃ H ₉ N ₂ O ₄ Zn	C ₂₈ H ₂₀ N ₄ O ₈ Zn ₂	C ₂₈ H ₂₂ N ₄ O ₈ Zn ₂	C ₂₉ H ₂₄ N ₄ O ₈ Zn ₂
fw	322.61	671.22	673.24	687.26
pattern range 2θ (deg)	6–80	5–80	5–80	5–80
step size Δ2θ (deg)	0.015 43	0.015 43	0.015 43	0.015 43
wavelength (Å)	1.540 598	1.540 598	1.540 598	1.540 598
cryst syst	monoclinic	monoclinic	monoclinic	orthorhombic
space group	<i>P2₁/c</i>	<i>C2/c</i>	<i>C2/c</i>	<i>Pna2₁</i>
<i>a</i> (Å)	11.58082(32)	25.9183(9)	26.0448(9)	16.0405(4)
<i>b</i> (Å)	7.70682(20)	7.43553(30)	7.44817(29)	7.65135(18)
<i>c</i> (Å)	15.9980(4)	16.2652(6)	16.2399(6)	25.1087(5)
α (deg)	90	90	90	90
β (deg)	107.6361(19)	113.1355(24)	113.3305(24)	90
γ (deg)	90	90	90	90
<i>V</i> (Å ³)	1360.74(6)	2882.47(20)	2892.74(19)	3081.64(12)
<i>Z</i>	4	4	4	4
no. of obsns	4817	4872	4872	4943
no. of reflns	856	965	949	1058
no. of refined param	92	94	97	160
<i>R_p</i>	0.0609	0.0342	0.0702	0.0423
<i>R_{wp}</i>	0.0789	0.0498	0.0948	0.0566
<i>R_f</i> ²	0.0756	0.0582	0.0772	0.0671

^a The calculated standard deviations are given in parentheses.

dimensions were followed by refinements of the atomic coordinates. The atomic coordinates were refined with soft constraints being introduced: $d(\text{C}-\text{C}) = 1.39(2)$ Å, $d(\text{C}-\text{N}) = 1.35(2)$ Å, and $d(\text{C}-\text{O}) = 1.26(2)$ Å. In addition, $d(\text{C}-\text{C}) = 2.41(3)$ Å and $d(\text{C}-\text{N}) = 2.39(3)$ Å were constrained in order to keep the angles in the aromatic rings near 120°. Isotropic displacement parameters were refined, and common parameters were adopted for C, N, and O. The contribution of the H atoms to the scattered intensity was neglected. The weight on the soft constraints could not be completely relaxed. For details of the refinements, see Table 2. The observed, calculated, and difference diffraction profiles from the refinements are shown in Figure 1.

Results and Discussion

Recently, Wu et al.²⁴ obtained a novel coordination polymer based on Zn and aip, $[\text{Zn}(\text{aip})(\text{H}_2\text{O})]_n$, by hydro-

thermal synthesis with water as the solvent. Its crystal structure contains infinite 2D layers with tetrahedral Zn atoms and aip ligands in a triangular topology (Figure 2a). Each Zn is coordinated to three different aip ligands through two monodentate carboxylate groups and one amino group. A terminal water molecule constitutes the fourth coordination bond of Zn. All terminal water molecules of a given layer are oriented in the same direction (Figure 2b). In the subsequent layer, the water molecules are oriented in the opposite direction. These layers are linked into pairs by strong H-bonding interactions.

By replacing water as a solvent in the synthesis reported by Wu et al. with a mixture of DEF and ethanol, we obtained

(24) Wu, C. D.; Lu, C. Z.; Yang, W. B.; Zhuang, H. H.; Huang, J. S. *Inorg. Chem.* **2002**, *41*, 3302.

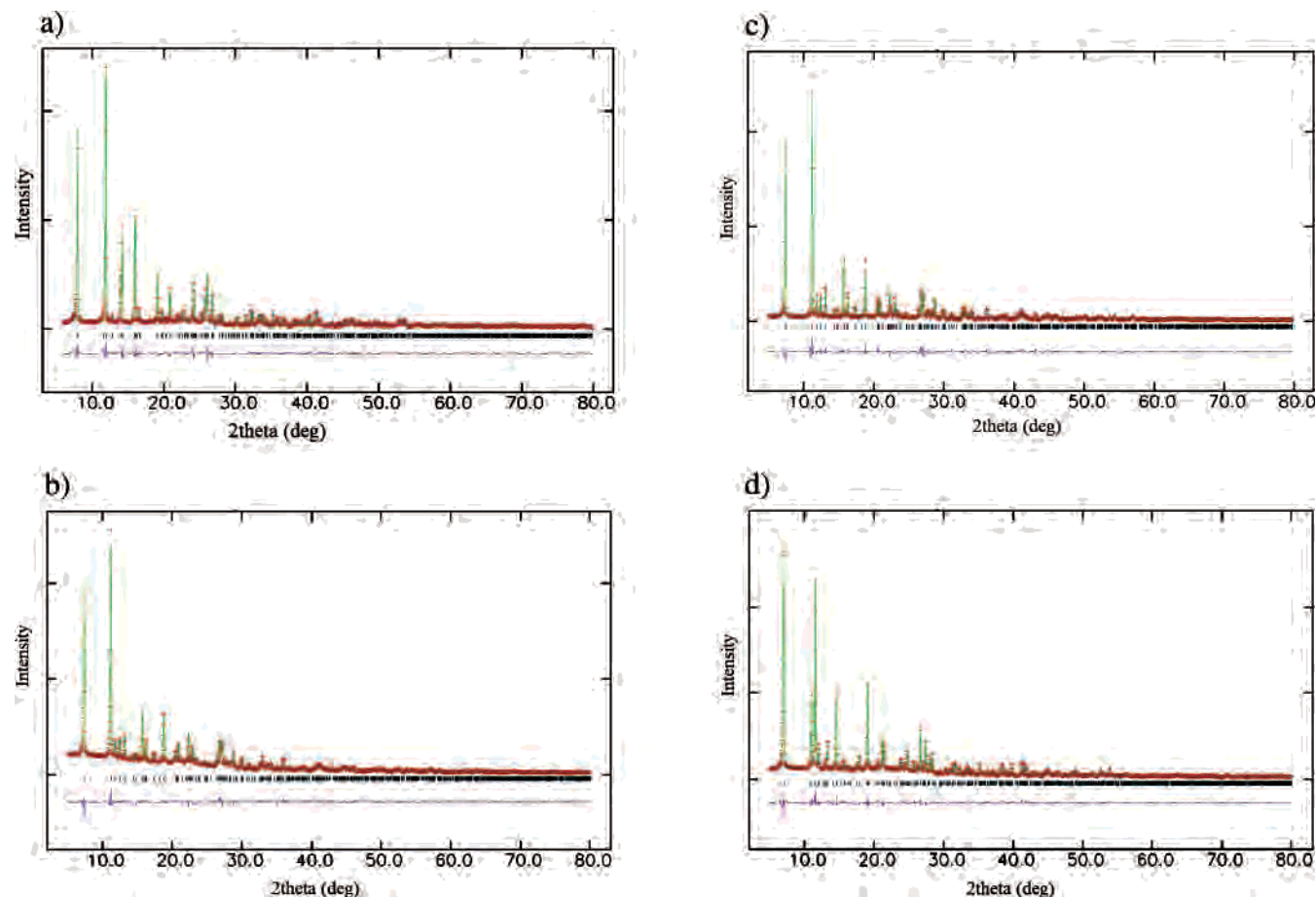


Figure 1. Observed, calculated, and difference powder X-ray diffraction profiles for (a) CPO-8-BPY, (b) CPO-8-DPE, (c) CPO-8-DPA, and (d) CPO-8-DPP.

a compound denoted as CPO-8-DEF, whose the crystal structure is related to that of $[\text{Zn}(\text{aip})(\text{H}_2\text{O})]_n$. In CPO-8-DEF, one finds the same type of 2D dense triangular layers; however, DEF molecules now replace the terminal water molecules. Within each layer, the DEF molecules are oriented in the same direction (Figure 3), while in the subsequent layer, the DEF molecules are oriented in the opposite direction. This leads to increased interlayer distance compared with that of $[\text{Zn}(\text{aip})(\text{H}_2\text{O})]_n$ simply because the more spacious DEF molecules replace the water molecules; see Figure 3. The layers are connected by H bonds between the amino groups of one layer and the carboxylate O atoms of the subsequent layer [$d(\text{N}\cdots\text{O}1) = 3.041(6) \text{ \AA}$ and $d(\text{N}\cdots\text{O}3) = 3.019(6) \text{ \AA}$]. The ethyl groups of the DEF molecules are disordered.

On the basis of synthetic reports and the crystal structures of $[\text{Zn}(\text{aip})(\text{H}_2\text{O})]_n$ and CPO-8-DEF, there are two distinct observations that act as guidelines for a more general route toward the construction of novel structures. First, the triangular layer appears as a preferred reaction product in reactions between Zn salts and the aip ligand under different synthetic conditions. Second, for this layer component, the fourth coordination bond around Zn is directed toward the interlamellar space and is exchangeable. By the introduction of bifunctional ligands into a synthetic system that forms Zn(aip) triangular layers, one would expect the formation of a pillared bilayer framework structure with 1D channels.

We have indeed discovered such a system. By the introduction of BPY, DPE, DPA, and DPP into mixtures of DMF and water with $\text{Zn}(\text{NO}_3)_2$ and aip, we have successfully synthesized a series of related pillared bilayer compounds with a common triangular Zn(aip) layer structural motif.

The crystal structure of CPO-8-BPY is a unique pillared bilayer structure. The same triangular layers as those identified in $[\text{Zn}(\text{aip})(\text{H}_2\text{O})]_n$ and CPO-8-DEF are present. The bilayers formed with BPY ligands as the connectors are stacked along the [100] direction (Figure 4). These bilayers are, furthermore, interconnected by H bonds between the amino groups and the carboxylate O atoms [$d[\text{N}(1)\cdots\text{O}(2)] = 3.049(3) \text{ \AA}$ and $d[\text{N}(1)\cdots\text{O}(3)] = 3.100(3) \text{ \AA}$]. The BPY pillars create spaces inside the bilayers that result in 1D channels running along the [010] direction with dimensions of $3.5 \times 6.7 \text{ \AA}^2$ (Figure 4). These channels contain three water molecules per formula unit. One of the water molecules is disordered over two positions. All of the water molecules are involved in an extensive H-bonding scheme that also involves the carboxylate O atoms.

The thermal stability of CPO-8-BPY was examined using TGA. The TGA curve indicates the release of water molecules up to $150 \text{ }^\circ\text{C}$ (obsd weight loss 10.5%; calcd 14.3%). The compound is stable up to $350 \text{ }^\circ\text{C}$, where a second weight loss starts that indicates decomposition of the organic ligands. The powder X-ray diffraction pattern of CPO-8-BPY dehydrated at $150 \text{ }^\circ\text{C}$ shows sharp diffraction

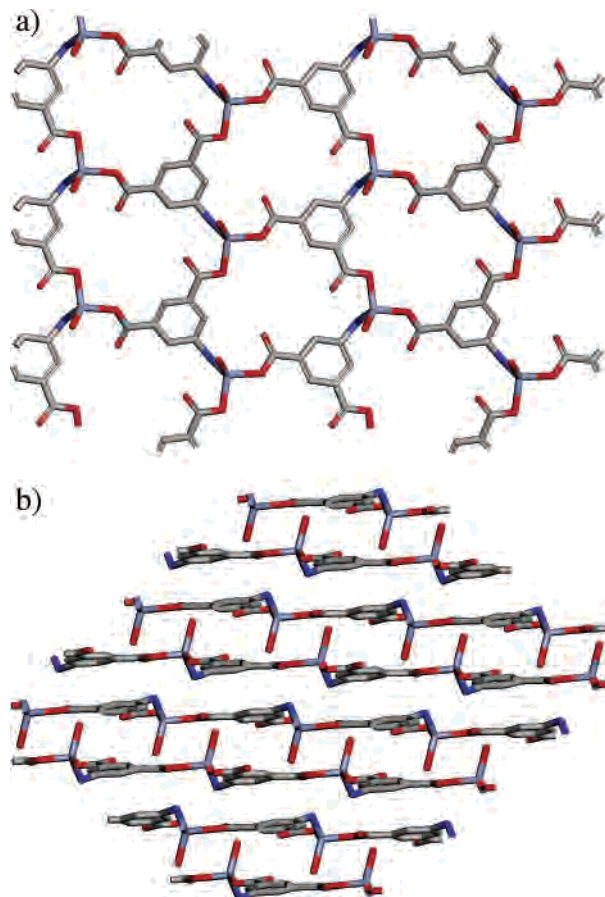


Figure 2. (a) Tetrahedral Zn and aip ligands linked into 2D layers in a triangular topology. (b) Stacking of 2D layers in $[\text{Zn}(\text{aip})(\text{H}_2\text{O})]_n$.

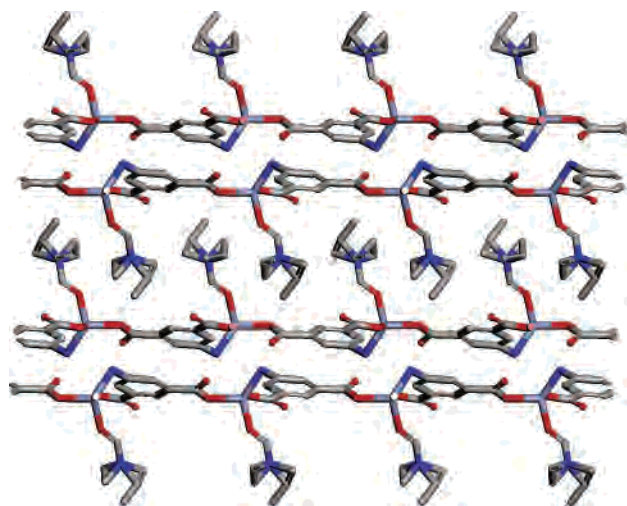


Figure 3. Stacking of 2D layers in CPO-8-DEF.

peaks, indicating that the framework is maintained even after removal of the water molecules from the channels. The Rietveld refinement analysis of the powder X-ray data confirmed that the framework is virtually unchanged after the dehydration, giving CPO-8-BPY-150 a porous structure. The free volume was estimated by the program PLATON²⁵ to be 20.7% of the unit cell volume, while the effective dimensions of the pores are $3.5 \times 6.7 \text{ \AA}^2$.

(25) Spek, A. L. *Acta Crystallogr., Sect A* **1990**, *46*, C34.

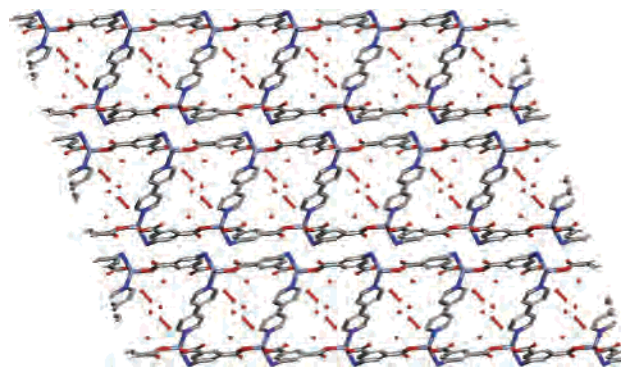


Figure 4. Stacking of bilayers along [100] in CPO-8-BPY.

It turned out to be possible to exchange the pillaring BPY module in CPO-8-BPY by either of three similar molecules, resulting in three new compounds in the CPO-8 series, namely, CPO-8-DPE, CPO-8-DPA, and CPO-8-DPP; see Figure 5. The increase in the length of the pillars from BPY to DPP does, however, not lead to any significant increase in the pore dimension along [010]. Actually, the orientation of the Zn tetrahedra forces the pillaring molecules into a bent position along [100] ([001] for CPO-8-DPP) and thus increases the pore dimensions along [001] ([100] for CPO-8-DPP) instead. The dimensions of the pores in this direction still remain small compared with the channels along [010].

The thermal properties of CPO-8-DPE, CPO-8-DPA, and CPO-8-DPP are similar to those of CPO-8-BPY. The TGA curves show two distinct weight losses. The first stage with a water loss from channels takes place up to 150 °C (CPO-8-DPE obsd weight loss 11.70%, calcd 11.83%; CPO-8-DPA obsd 10.71%, calcd 11.80%; CPO-8-DPP obsd 11.60%, calcd 13.59%). Thermal decomposition of the frameworks starts around 350 °C. Analogous to CPO-8-BPY, dehydrated samples at 150 °C appear as porous on the basis of powder X-ray patterns with sharp reflections. Rietveld analyses of such diffraction data confirmed for all three compounds that the frameworks are virtually unchanged after the dehydrations, resulting in porous structures with the following free volumes: CPO-8-DPE, 23.5%; CPO-8-DPA, 23.5%; CPO-8-DPP, 25.5%.

The isotherms of N_2 measured at 77 K for the CPO-8 types of compounds showed no sorption for any of the compounds. However, at the same temperature, a small but significant sorption of H_2 was observed for all of the compounds. This preferential sorption of H_2 over N_2 is shown for CPO-8-DPP in Figure 6. The uptake of H_2 at 1 atm was as follows: CPO-8-BPY, $11.3 \text{ cm}^3(\text{STP})/\text{g}$ (0.093 wt %); CPO-8-DPE, $9.6 \text{ cm}^3(\text{STP})/\text{g}$ (0.079 wt %); CPO-8-DPA, $10.8 \text{ cm}^3(\text{STP})/\text{g}$ (0.089 wt %); CPO-8-DPP, $24.0 \text{ cm}^3(\text{STP})/\text{g}$ (0.197 wt %). The H_2 uptake for CPO-8-DPP is in the same range as that for the MOF structure CPL-1,²⁶ while the uptake for the other compounds is similar to the uptake of the nanoporous nickel phosphate VSB-1.²⁷ Preferential adsorption of H_2 over N_2

(26) Kubota, Y.; Takata, M.; Matsuda, R.; Kitaura, R.; Kitagawa, S.; Kato, K.; Sakata, M.; Kobayashi, T. C. *Angew. Chem., Int. Ed.* **2005**, *44*, 920.

(27) Forster, P. M.; Eckert, J.; Chang, J. S.; Park, S. E.; Ferey, G.; Cheetham, A. K. *J. Am. Chem. Soc.* **2003**, *125*, 1309.

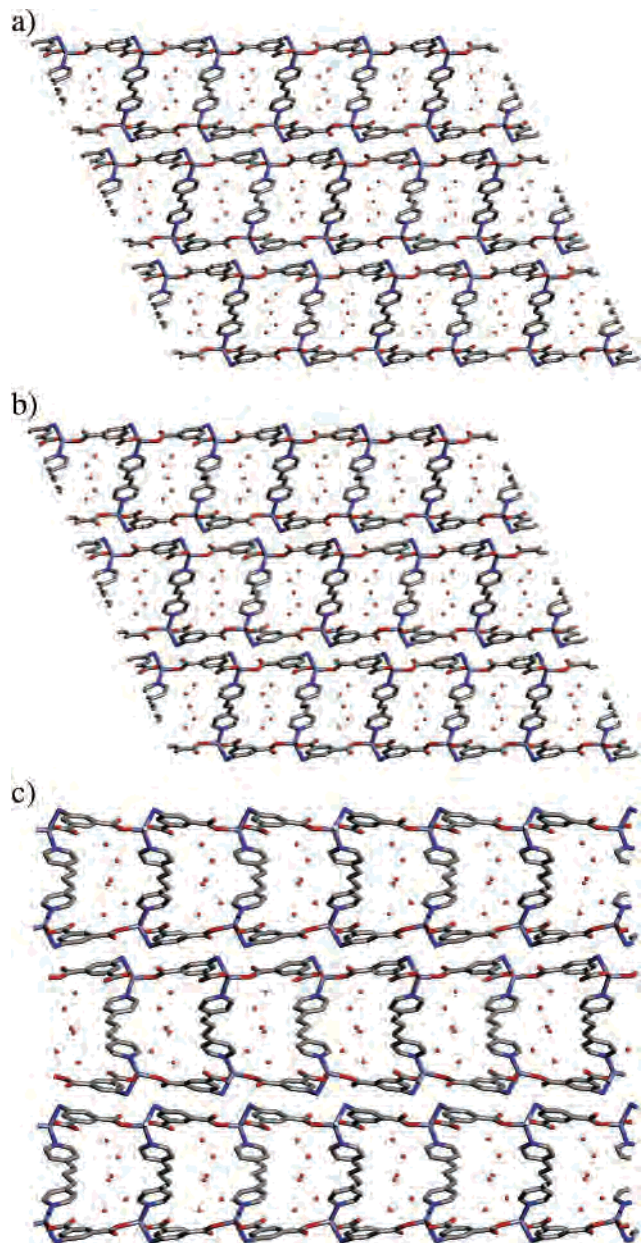


Figure 5. Stacking of bilayers along [100] in (a) CPO-8-DPE and (b) CPO-8-DPA and along [001] in (c) CPO-8-DPP.

in MOF compounds has just been observed before for Mn-(HCO₂)₂²⁸ and Mg₃ndc₃²⁹ (ndc = 2,6-naphthalenedicarboxylate). This behavior may be explained by the fact that the apertures of the channels are too small to allow N₂ molecules to enter because the kinetic diameters of the molecules³⁰ (3.64

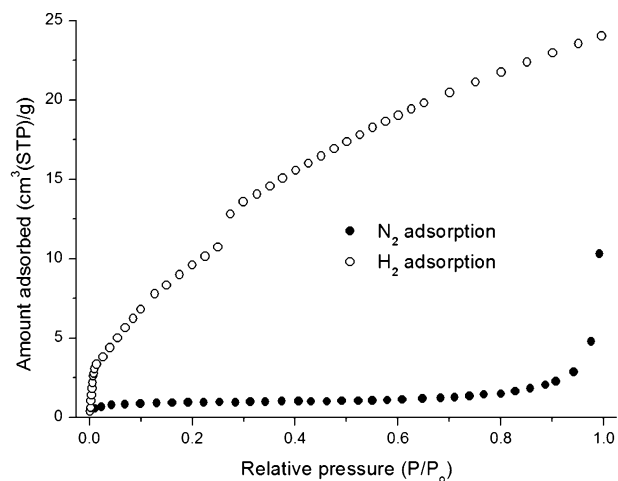


Figure 6. N₂ and H₂ gas sorption isotherms at 77 K for CPO-8-DPP. P/P_0 is the ratio of the gas pressure (P) to the saturation pressure (P_0), with $P_0 = 1.0$ bar.

Å) are larger than the smallest channel aperture size (3.5 Å). The kinetic diameter of H₂ of 2.8 Å³⁰ is, however, small enough for the molecules to enter the channels.

Conclusion

In conclusion, the CPO-8 series of compounds demonstrate the use of a unique, pillared bilayer motif for the rational synthesis of novel porous coordination polymers. This approach will allow the construction of novel coordination polymers with the potential for various applications because modification of the pillaring ligands may enable systematic control of the pore size as well as pore functionality.

Acknowledgment. This work has received support from the Research Council of Norway, Project No. 151502, as part of the Klimatek research effort. Dr. Richard Blom and Aud I. Spjelkavik at SINTEF are thanked for performing the H₂ sorption isotherm experiments.

Supporting Information Available: X-ray crystallographic data in CIF format. This material is available free of charge via the Internet at <http://pubs.acs.org>.

IC050662V

(28) Dybtsev, D. N.; Chun, H.; Yoon, S. H.; Kim, D.; Kim, K. *J. Am. Chem. Soc.* **2004**, *126*, 32.

(29) Dinca, M.; Long, J. R. *J. Am. Chem. Soc.* **2005**, *127*, 9376.

(30) Beck, D. W. *Zeolite Molecular Sieves*; John Wiley & Sons: New York, 1974.